Cascades in decaying three-dimensional electron magnetohydrodynamic turbulence

CHRISTOPHER J. WAREING
and RAINER HOLLERBACH

Department of Applied Mathematics, University of Leeds,
Woodhouse Lane, Leeds, LS2 9JT, UK
(cjw@maths.leeds.ac.uk)

Abstract. Decaying electron magnetohydrodynamic (EMHD) turbulence in three dimensions is studied via high-resolution numerical simulations. The resulting energy spectra asymptotically approach a k^{-2} law with increasing R_B, the ratio of the nonlinear to linear time scales in the governing equation, consistent with theoretical predictions. No evidence is found of a dissipative cutoff, consistent with non-local spectral energy transfer and recent studies of 2D EMHD turbulence. Dissipative cutoffs found in previous studies are explained as artificial effects of hyperdiffusivity. In another similarity to 2D EMHD turbulence, relatively stationary structures are found to develop in time, rather than the variability found in ordinary or MHD turbulence. Further, cascades of energy in 3D EMHD turbulence are found to be suppressed in all directions under the influence of a uniform background field. Energy transfer is further reduced in the direction parallel to the field, displaying scale-dependent anisotropy. Finally, the governing equation is found to yield a weak inverse cascade, at least partially transferring magnetic energy from small to large scales.

1. Introduction

Turbulence plays a crucial role in a wide variety of geophysical and astrophysical fluid flows. In this paper we present results on a specific variety of plasma turbulence in which the flow consists entirely of electrons, moving through a static background of ions. The equation governing the electrons' self-induced magnetic field is then

$$\frac{\partial \mathbf{B}}{\partial t} = -\nabla \times [\mathbf{J} \times \mathbf{B}] + R_B^{-1} \, \nabla^2 \mathbf{B}, \tag{1.1}$$

where $\mathbf{J} = \nabla \times \mathbf{B}$ and $R_B = \sigma B_0 / nec$, with σ the conductivity, B_0 a measure of the field strength, n the electron number density, e the electron charge and c the speed of light. See for example Goldreich and Reisenegger (1992), who derived this equation in the context of magnetic fields in the crusts of neutron stars. More generally though, it is applicable in many weakly collisional, strongly magnetic plasmas, so other applications could include the Sun's corona or the Earth's magnetosphere.

Turbulence governed by (1.1) is known as electron MHD (EMHD), Hall MHD or whistler turbulence. Based on its (at least superficial) similarity to the vorticity

equation governing ordinary, non-magnetic turbulence,

$$\frac{\partial \mathbf{w}}{\partial t} = \nabla \times [\mathbf{u} \times \mathbf{w}] + Re^{-1}\nabla^2\mathbf{w}, \tag{1.2}$$

where now $\mathbf{w} = \nabla \times \mathbf{u}$, Goldreich and Reisenegger (1992) argued that (1.1) would initiate a turbulent cascade to small length scales, thereby accelerating neutron stars' magnetic field decay beyond what ohmic decay acting on large length scales could achieve. They suggested in particular that the turbulent spectrum would scale as k^{-2}, with a dissipative cutoff occurring at $k \sim R_B$.

However, recent work has highlighted the fundamental differences between (1.1) and (1.2) (Wareing and Hollerbach 2009, henceforth referred to as WH09). In (1.2) the dissipative term contains more derivatives than the nonlinear term, so on sufficiently short length scales the dissipative term will always dominate and hence there is a dissipative cutoff. In contrast, in (1.1) the two terms both contain two derivatives, so it is conceivable that the nonlinear term will always dominate, even on arbitrarily short length scales. WH09 found precisely this effect in decaying two-dimensional (2D) EMHD turbulence.

In this paper we present high-resolution numerical simulations of (1.1) in a three-dimensional (3D) periodic box geometry, designed specifically to address such questions as to whether there is a dissipative cutoff or not, and whether the coupling is local or not. In contrast to previous 3D simulations (Biskamp et al. 1999; Biskamp and Müller 1999; Cho and Lazarian 2004), we do not employ hyperdiffusivity, which disrupts the feature that the two terms in (1.1) have the same number of derivatives, and hence introduces an artificial dissipative cutoff (WH09). These previous simulations found no difference between 2D and 3D turbulent spectra, with both having a $k^{-7/3}$ scaling. In our recent study of the governing equation in two dimensions with normal diffusivity (WH09), we found no evidence for a dissipative cutoff, and the turbulent spectrum scaled as $k^{-5/2}$, broadly consistent with previous results. We now consider whether 3D EMHD turbulence displays the same scaling characteristics. Finally, we also consider the question of whether (1.1) is capable of yielding an inverse cascade in 3D (we use hyperdiffusivity for this set of runs).

2. Numerics

We solve (1.1) by treating the z-independent parts of $\mathbf{B}$ as before (WH09). For the z-dependent parts we expand B_x and B_y in triple Fourier series in x, y and z, with B_z then given by $\nabla \cdot \mathbf{B} = 0$. Time integration is achieved through a second-order Runge–Kutta method, with the diffusive term treated exactly. We employ standard pseudospectral techniques for the evaluation of the nonlinear terms, with dealiasing according to the 2/3 rule. The code employs the MPI library (http://www.mcs.anl.gov/mpi/) and the FFTW library (Frigo and Johnson 2005) to achieve massive parallelisation on a suitable supercomputer. We performed a variety of runs, typically employing 64 processors, with the highest extending to $k = 170$ in Fourier space, corresponding to $N = 512$ collocation points in real configuration space. Due to the two derivatives in the nonlinear term, the required time steps are unfortunately very small, roughly proportional to $1/N^2$. Values as small as $\sim 1 \times 10^{-6}$ were used, requiring $O(2 \times 10^5)$ time steps to reach $t = 0.2$.

2.1. Initial conditions

Since our interest is in freely decaying, rather than forced, turbulence, we need to carefully consider the nature of our chosen initial conditions. We will present results for three different sets of runs.

First, to study homogeneous forward cascades, we start off with random $O(1)$ energies in all Fourier modes up to $k = (k_x^2 + k_y^2)^{1/2} = 5$, making sure that the energy is evenly distributed between the three components. After initialisation the overall amplitude of the field is rescaled to ensure that the rms value of $|\mathbf{B}|$ is 1 at $t = 0$.

Second, to study non-homogeneous forward cascades, we start off with the same initialisation as above, but now add a uniform field $C\hat{\mathbf{e}}_x$, where $C = 1$, 2, 4 or 8. This field is simply added to the B_x component directly, resulting in a suitably modified equation (1.1).

Third, to explore the possibility of inverse cascades, we return to the $C = 0$ case without any large-scale magnetic field and now inject energy into modes in the range $10 \leqslant k \leqslant 20$. The question then is how much of this initial energy moves to $k < 10$, and how much moves to $k > 20$.

Finally, for all three sets of results, each individual run was repeated with a number of different random initial conditions, to ensure that the results presented here are indeed representative.

2.2. Ideal invariants

Equation (1.1) has some useful associated diagnostics, corresponding to quantities that are conserved in the ideal, $R_B^{-1} \to 0$, limit. Specifically, in three dimensions we have equations for the energy,

$$\frac{d}{dt}\frac{1}{2}\int \mathbf{B}^2 \, dV = -R_B^{-1}\int \mathbf{J}^2 \, dV, \tag{2.1}$$

and the magnetic helicity,

$$\frac{d}{dt}\frac{1}{2}\int \mathbf{A}\cdot\mathbf{B} \, dV = -R_B^{-1}\int \mathbf{B}\cdot\mathbf{J} \, dV, \tag{2.2}$$

where $\mathbf{A}$ is the vector potential, defined by $\mathbf{B} = \nabla \times \mathbf{A}$. Note though that in the presence of a uniform background field, helicity is not even defined (Berger 1997), let alone conserved.

Whereas in two dimensions, we also had the additional quantity of the mean squared magnetic potential or anastrophy, this is not conserved in three dimensions. This quantity is particularly important for the inverse cascade in 2D EMHD, where such a cascade is thought to be driven by a forward cascade of energy and an inverse cascade of anastrophy (Shaikh and Zank 2005). It is unclear, then, whether an inverse cascade will occur in 3D.

In addition to the physical insight that these various integrated quantities yield into the nature of the Hall nonlinearity, they also offer useful diagnostic checks of the code. Reassuringly, we found that both of them (except helicity in a uniform field) were satisfied to within 0.25% or better by all of our runs.
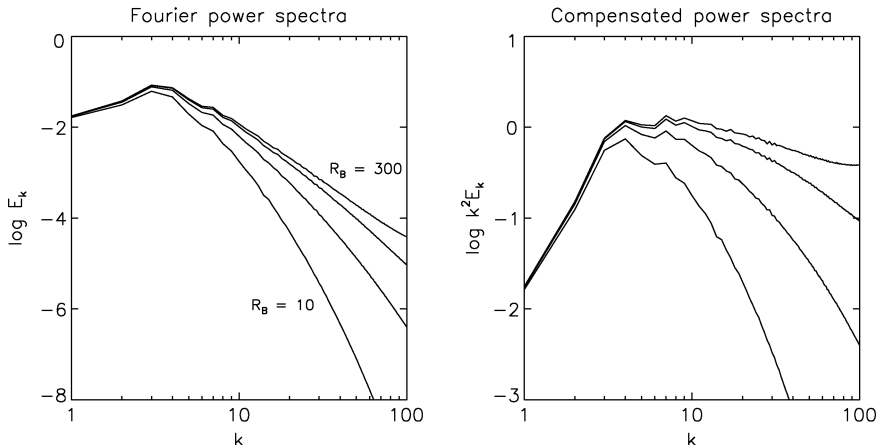
Figure 1. Energy spectra of homogeneous 3D EMHD turbulence at $t = 0.2$. On the left are shown spectra for $R_B = 10, 30, 100$ and 300. On the right, compensated spectra $k^2 E_k$ for the same range of R_B.

3. Results

3.1. Large-scale initial conditions

A characteristic statistical quantity of a turbulent system is the energy spectrum. Three-dimensional hydrodynamic turbulence exhibits the spectrum $E_k \propto k^{-5/3}$, the famous Kolmogorov law (Kolmogorov 1941). In MHD turbulence, the energy transfer is altered by the Alfvén effect (Iroshnikov 1964; Kraichnan 1965), leading to a flatter energy spectrum $E_k \propto k^{-3/2}$. Recent studies of 2D EMHD turbulence have found, via methods which all employ hyperdiffusivity, a 5/3 Kolmogorov spectrum for small scales $k d_{\mathrm{e}} > 1$, equivalent to $k > O(R_B)$, and a steeper 7/3 spectrum for longer wavelengths (Biskamp et al. 1996, 1999; Cho and Lazarian 2004; Dastgeer et al. 2000; Dastgeer and Zank 2003; Shaikh and Zank 2005). Of the studies which considered 3D EMHD turbulence, Biskamp et al. (1999) numerically found a scaling of 7/3 for $k d_{\mathrm{e}} < 1$ consistent with a local spectral energy transfer independent of the linear wave properties. However, the authors of that paper noted the scaling in 3D was only marginally verified, since the short extent of the inertial spectral range was dominated by the bottleneck effect, causing local enhancement of the spectrum above the inertial range power law at the point of transition from the inertial range to the dissipation range. The more abrupt the transition (or the higher the degree of hyperdiffusivity), the more pronounced the effect.

In the left-hand plot of Fig. 1, we show the energy spectra of our solutions for $R_B = 10, 30, 100$ and 300, evolved to a time $t = 0.2$. The energy spectra have been stationary since approximately $t = 0.16$ and time averaging between 0.16 and 0.2 reveals an identical spectrum and no further information. We interpret this to mean that our simulations are resolved and evolved to a suitable time for inspection of the now quasi-stationary cascade. It is worth noting at this point that 3D EMHD turbulence takes a longer time to reach quasi-stationarity than 2D EMHD turbulence, which achieves such a phase by $t \approx 0.1$.

The energy spectra all start out much the same at low k, peak around $k = 3$ and then lower-R_B spectra smoothly drop off with increasing k whilst higher-R_B spectra maintain a linear gradient in the log–log plot. Transfer of energy to higher

k is then more efficient at higher R_B, with $R_B = 300$ having a scaling of $\sim k^{-5/2}$. The spectra are asymptotically approaching an energy spectrum $E_k \propto k^{-\nu}$, where we propose that $\nu \sim 2$. In the right-hand plot of Fig. 1, we show compensated energy spectra to show this approach to $k^2 E_k = 1$ with increasing R_B. Our value of ν is the same as that predicted by Goldreich and Reisenegger (1992) for 3D EMHD turbulence. Their prediction was calculated using a phenomenology based on Kraichnan's arguments (the whistler effect) and is reproduced in Biskamp et al. (1996). Biskamp et al. (1996) also considered a theoretical prediction neglecting the whistler effect and derived a scaling of 7/3. Simulations have shown that the whistler effect has little effect on the energy spectrum of 2D EMHD turbulence, but it would seem that it may have a considerable effect on 3D EMHD turbulence.

Regarding the bottleneck effect, we see no evidence for it in the spectra. This is not a great surprise as we see no sign of a dissipative cutoff, which causes the effect. By definition, the dissipation scale should occur when the local value of R_B is $O(1)$ in (1.1). It is unclear though when this occurs, since the definition of R_B does not involve length scales. If the coupling is purely local in wavenumber, then this definition does involve length scales after all, since the B_0 that should be used is the field at that wavenumber only, rather than the total field. That is, according to the definition of Hollerbach and Rüdiger (2002) where this argument was first developed, we have

$$R'_B = R_B(B'/B),\qquad(3.1)$$

where the primed quantities are the small-scale local values and the unprimed the large-scale global values. If we now suppose a k^{-2} energy spectrum, then $B'/B \sim k^{-1}$ and so R'_B is reduced to $O(1)$ when $k \sim R_B$. So, at $R_B = 100$ we would see a dissipative cutoff at $k \sim 100$, which we do not. It is possible to reconcile the situation by realising that this argument crucially depends on the coupling being local in Fourier space: if this does not hold, then $R'_B = R_B$ and there is simply no definite dissipation scale.

In agreement then with our 2D study of EMHD turbulence, the nonlinear term is able to dominate at all length scales and the coupling is therefore non-local in Fourier space. Again, hyperdiffusivity has previously masked the effect of the nonlinear term at high k. It has also introduced the bottleneck effect, which has disguised the true scaling of the energy spectra. With normal diffusivity, we believe that we have performed the first true simulations of 3D EMHD turbulence.

In Fourier space, then, EMHD turbulence continues to bear a strong resemblance to ordinary MHD turbulence. We would like to know if this resemblance carries over into real configuration space. In Fig. 2, we show slices through the three component field datacubes at $t = 0.1$. Across the top row, we show a slice of the B_x field at $x = 0.5$ on the left, a slice at $y = 0.5$ in the middle and a slice at $z = 0.5$ on the right. Across the middle row we show the same slices for B_y and across the bottom row for B_z. Large numbers of small, independent vortices dominate the fields, characteristic of fully developed turbulence.

In Fig. 3, we show the same fields at $t = 0.2$. It is clear that the fields resemble those at $t = 0.1$, implying that 3D EMHD turbulence is much more structured than classical and MHD turbulence, where a fully developed turbulent field would bear no resemblance to the initial field. This appears to be a unique characteristic of decaying EMHD turbulence, in both two and three dimensions.
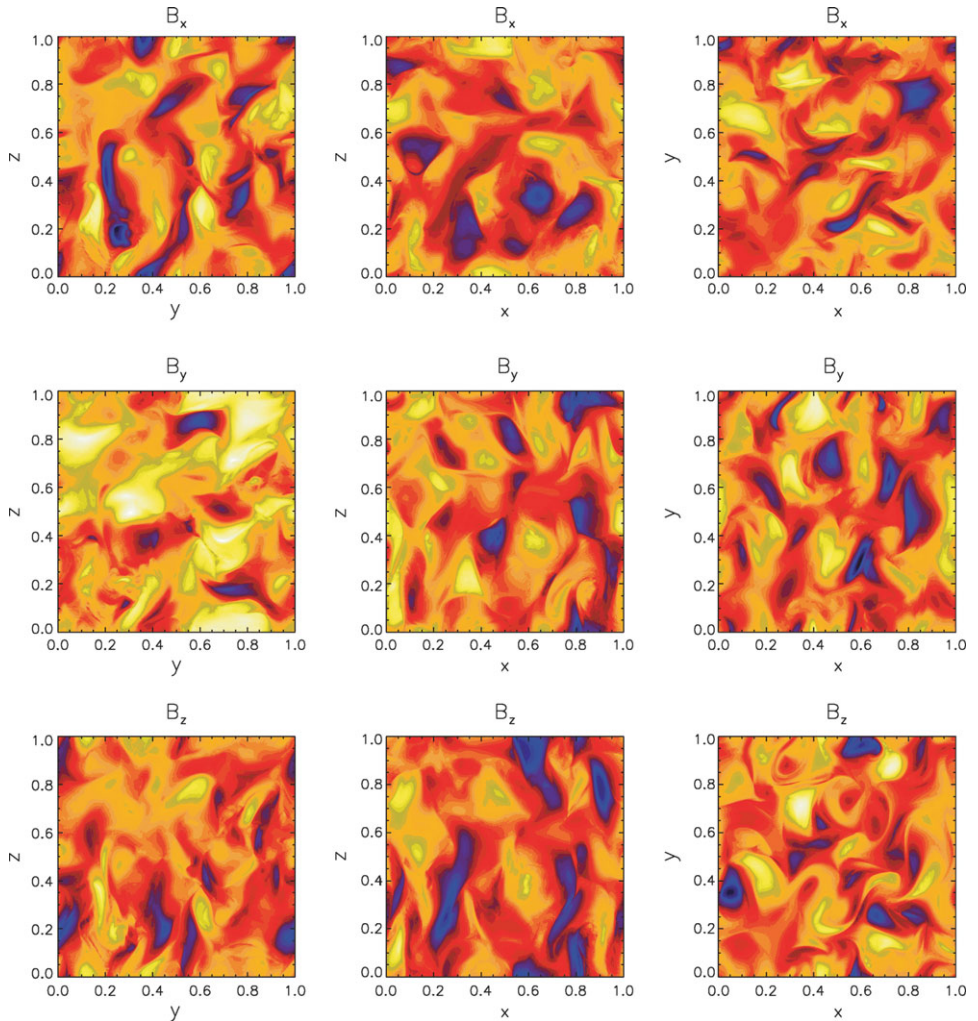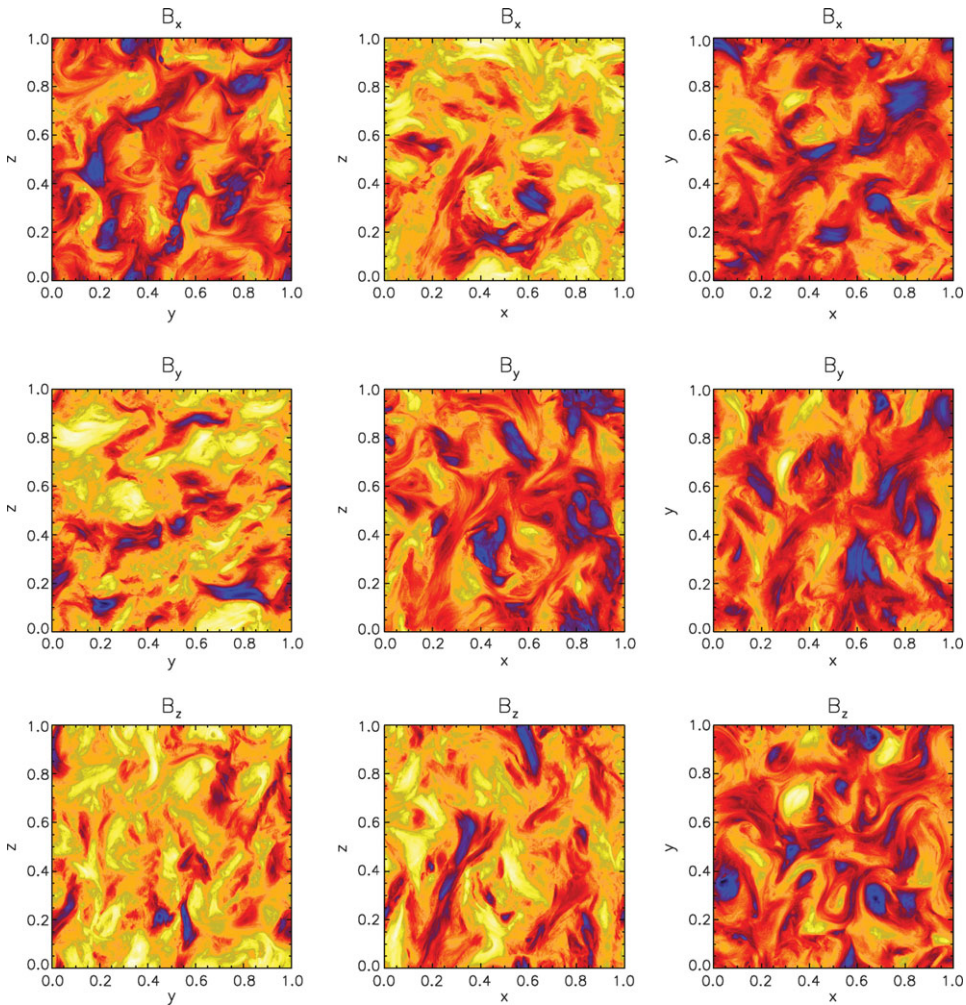
Figure 2. Plots of the $R_B = 300$ solution in real configuration space at $t = 0.1$. For full details of the slices through the datacubes, see the text (a colour version of this figure is available online at www.journals.cambridge.org/pla).

We would also like to address the energy decay of the field, with particular respect to any dependency of the decay rate on the value of R_B. Biskamp and Müller (1999) reported that the energy dissipation rate is independent of the value of the dissipation coefficient, represented by R_B here. In contrast, WH09 found that the energy decay is strongly dependent on the R_B parameter, with the decay rate proportional to R_B^{-1}. We find the same behaviour here, as shown in Fig. 4.

### 3.2. Large-scale initial conditions in the presence of a background field

Three-dimensional EMHD turbulence, like 2D EMHD and classical and MHD turbulence, is isotropic when allowed to freely decay. In the presence of a background flow, classical turbulence remains isotropic. Small-scale structures are advected along by any large-scale flow, whether or not that has a uniform background

Figure 3. Plots of the $R_B = 300$ solution in real configuration space at $t = 0.2$. For full details of the slices through the datacubes, see the text (a colour version of this figure is available online at www.journals.cambridge.org/pla).

contribution. This effect has been attributed to local coupling in phase space. Numerical simulations of MHD turbulence have found it to be strongly anisotropic in the presence of a background field (Shebalin et al. 1983; Oughton et al. 1998). This has been attributed to the excitation of Alfvén waves which preferentially propagate parallel to the external magnetic field and hinder the cascade process perpendicular to the external field.

In 2D EMHD turbulence, recent numerical studies employing hyperdiffusivity (Dastgeer et al. 2000; Dastgeer and Zank 2003) have revealed anisotropic behaviour with the cascade strongly inhibited parallel to the background field. This can only be the result of asymmetry in the nonlinear spectral transfer process relative to the external magnetic field. In the context of local energy coupling in Fourier space, mediation by whistler waves has been proposed as the only way this asymmetry
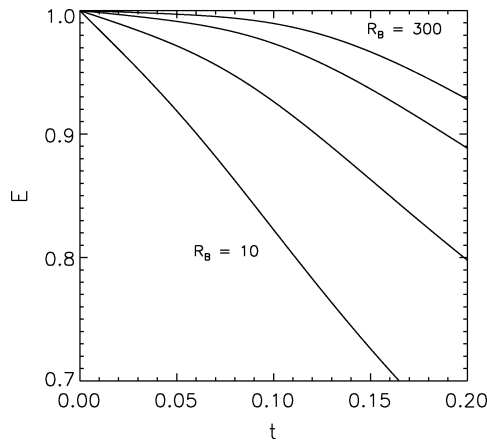
Figure 4. A plot of energy against time for $R_B = 10$, 30, 100 and 300, increasing from left to right.

could be achieved (Dastgeer et al. 2000), by the mechanism detailed by Galtier (2006). Most recently, the numerical study of WH09 has confirmed the anisotropy of 2D EMHD with normal diffusivity. The spectrum of 2D anisotropic EMHD turbulence has also been shown to exhibit a linear relationship with an external magnetic field (Dastgeer and Zank 2003, WH09).

In order to understand how hyperdiffusivity has affected previous studies, we have introduced a background field into the governing equations as discussed above and calculated solutions for $R_B = 100$ at a spatial resolution of 256^3 points in real configuration space. We present our results in Fig. 5. From left to right, we show 2D energy spectra for $R_B = 100$ with $C = 0$, 1, 2, 4 and 8. In the isotropic case with no background field, i.e. $C = 0$, energy is evenly distributed between x and y, as indicated by circular contours. In the case of $C = 1$ we find that energy transfer to larger k has been suppressed in the x direction, parallel to the background field. Three-dimensional decaying EMHD turbulence has become anisotropic in the presence of a uniform background field with normal diffusivity. The effect becomes more pronounced for $C = 2$ and particularly strong for $C = 4$ and $C = 8$. It is at these high values of C that the cascade is almost turned off in the direction parallel to the field and even strongly suppressed in the perpendicular directions. In 2D this suppression has been attributed to excitation of whistler waves, which act to weaken spectral transfer along the direction of propagation (Dastgeer and Zank 2003). In Fig. 6 we show a slice through the real configuration space field B_x at $z = 0.5$. For $C = 0$, the field is isotropic but, as the value of C is increased, structures stretch in the x direction corresponding to increasingly inhibited energy transfer in the x direction but not in y. We find the same for x compared to z. At $C = 8$, the structures have remained almost the same as at $t = 0$, since the cascade in all directions has been so strongly inhibited.

Cho and Lazarian (2004) performed 3D simulations of EMHD turbulence. They introduced a uniform background field of strength comparable to that of the fluctuating freely decaying field (i.e. $C = 1$). The authors employed a hyperdiffusivity of 3 and found scale-dependent anisotropy. Our simulation at $C = 1$ supports their result. Further, our simulations imply that the linear relationship between EMHD
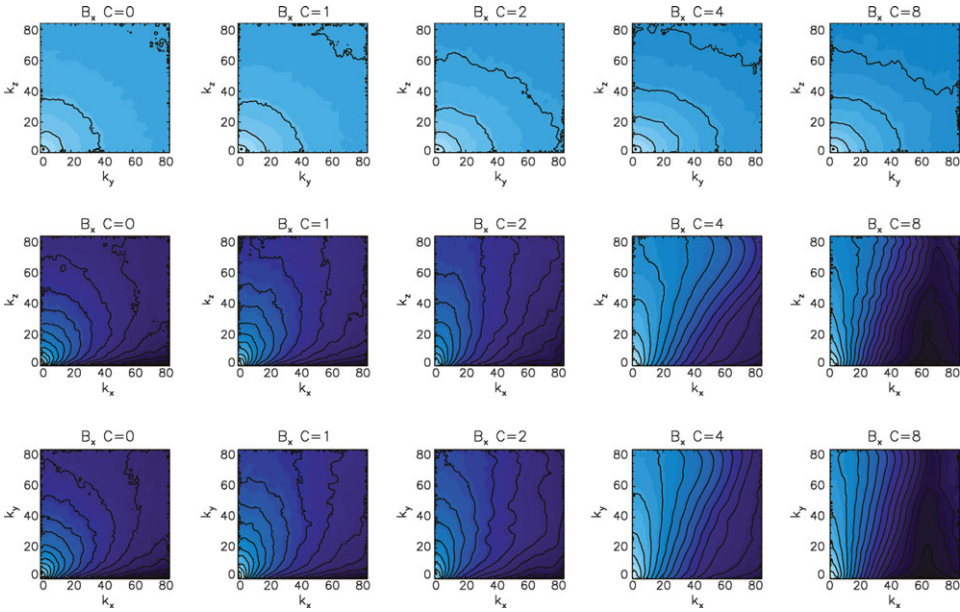
Figure 5. Two-dimensional Fourier power spectra at $t = 0.2$ for 3D EMHD turbulence in the presence of a background field. We show three 2D Fourier power spectra slices of the B_x datacube, at $k_x = 1$ (top row), $k_y = 1$ (middle row) and $k_z = 1$ (bottom row). Across the columns we show the power spectra for $C = 0, 1, 2, 4$ and 8 (a colour version of this figure is available online at www.journals.cambridge.org/pla).
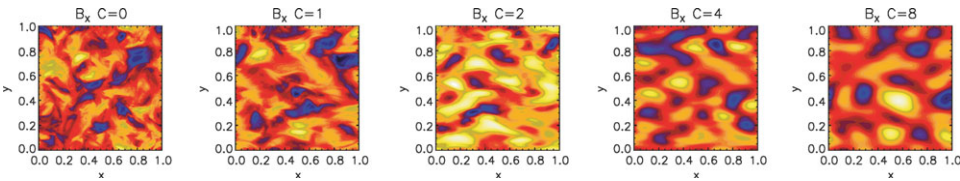
Figure 6. Slices of real configuration space B_x fields at $t = 0.2$ for 3D EMHD turbulence in the presence of a background field. From left to right, we show the fields for $C = 0$, $1, 2, 4$ and 8. In all cases $z = 0.5$ (a colour version of this figure is available online at www.journals.cambridge.org/pla).

turbulence and strength of the external magnetic field found by Dastgeer and Zank (2003) in 2D can be extended to 3D.

Note that (1.1) is scale invariant, i.e. it is possible to apply the equation over the whole of a system, or just to a small section, with R_B unchanged. A very small box then will see the large-scale field as a background field, and therefore the smallest scales in the system, for example a neutron star, should be anisotropic.

3.3. Intermediate-scale initial conditions

In 2D classical turbulence, the exchange of energy and enstrophy Ω is coupled in Fourier space according to

$$\frac{\partial E}{\partial t} = -k^2 \frac{\partial \Omega}{\partial t}; \qquad (3.2)$$

hence, energy injected at intermediate scales experiences a transfer to both higher and lower wavenumbers in order to satisfy this coupling and simultaneously conserve energy and enstrophy. This is the inverse cascade of energy to lower k (larger scales) (Kraichnan 1967). In MHD turbulence, energy and magnetic helicity are coupled in the same way and an inverse cascade occurs in order to simultaneously conserve these two quadratic ideal invariants. In driven 2D EMHD turbulence, the inverse cascade found by Shaikh and Zank (2005) has been proposed to be the result of simultaneous conservation of energy and mean squared magnetic potential, or anastrophy. Our recent simulations (WH09) have shown that an inverse cascade occurs in freely decaying 2D EMHD turbulence. Whilst it has a considerably different scaling nature to driven 2D EMHD turbulence, we believe that it is also the result of simultaneous conservation of energy and anastrophy. In 3D, then, the existence of an inverse cascade is immediately under question, since anastrophy is no longer conserved. We inject energy over the wavenumber range $10 \leqslant k \leqslant 20$ as detailed above and evolve the magnetic field to assess what inverse cascade there is, if any.

In this case, we have found that simulations with normal diffusivity are unable to produce an inverse cascade. Since the values of R_B available to us are considerably less than $R_B = 1000$, where decaying 2D EMHD turbulence displays an inverse cascade, this is not a surprising result. For the runs in this section we therefore introduce a hyperdiffusivity, so that the large scales see a diffusivity equivalent to $R_B > 1000$, whereas the small scales are much more strongly damped, so that the computations can be done at all. As noted above, using a hyperdiffusivity will of course disrupt features like the precise shape of the spectrum at large k, including the presence or absence of a dissipative cutoff. However, since here we are interested in the behaviour at more modest k, in particular the possibility of transferring energy from intermediate to small wavenumbers, these distortions at large k probably do not have that much effect on the results.

The precise form of the hyperdiffusivity is simply to raise the power of the diffusion operator,

$$\frac{\partial \mathbf{B}}{\partial t} = -\nabla \times [\mathbf{J} \times \mathbf{B}] - \epsilon(\nabla^2)^2 \mathbf{B}, \tag{3.3}$$

where ϵ is the new diffusion coefficient, the equivalent of R_B^{-1}, but only as seen by the largest scales.

Figure 7 shows spectra at $t = 0, 0.01, 0.02, 0.03$ and 0.04. The spectra show that energy is transferred to $k < 10$ in a very weak inverse cascade. The spectral peak is slowly shifting to $k < 10$ but not maintaining the same amplitude. Some energy has also been transferred to $k > 20$. In 3D, then, any inverse cascade is considerably weaker than in 2D, presumably since anastrophy is no longer conserved.

4. Conclusions

We have investigated the nature of decaying 3D EMHD turbulence with normal diffusivity and compared it with classical and MHD turbulence and studies of 2D and 3D EMHD with hyperdiffusivity. We have found that 3D EMHD turbulence experiences an isotropic forward cascade of energy to higher wavenumbers (smaller spatial scales) asymptotically approaching $E_k \propto k^{-2}$ with increasing R_B (inversely proportional to a dissipation coefficient). This is in agreement with the original
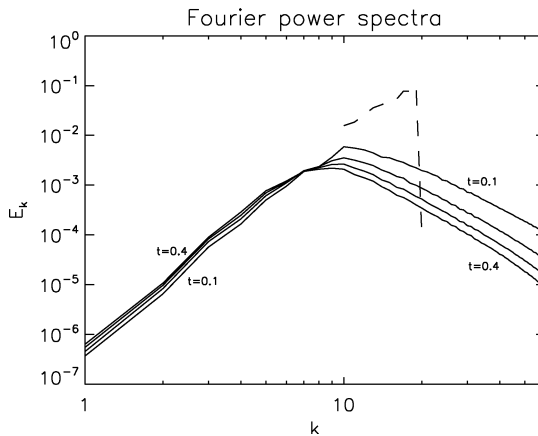
Figure 7. Time evolution of the Fourier power spectra for $\epsilon = 2.5 \times 10^{-6}$. Shown are power spectra at $t = 0, 0.01, 0.02, 0.03$ and 0.04. No further inverse cascade develops after $t = 0.04$.

theoretical prediction of Goldreich and Reisenegger (1992), suggesting that freely decaying 3D EMHD turbulence is mediated by whistler waves. Unlike the theoretical prediction, we have found that there is no dissipative cutoff at the predicted wavenumber $k \sim R_B$ and argue that this is consistent with non-local coupling in Fourier space, the most important result of this paper and consistent with our recent results for 2D EMHD turbulence. Hyperdiffusivity has previously clouded this issue and introduced an artificial cutoff and the unwanted bottleneck effect. We have also found that fully developed 3D EMHD turbulence appears to be strongly structured, retaining a similarity to the initial field at late times, very much unlike classical or MHD turbulence.

Three-dimensional EMHD turbulence with normal diffusivity has been found to display scale-dependent anisotropy in the presence of a uniform background field, in agreement with previous studies employing hyperdiffusivity. Our results support previous studies which found that the strength of the anisotropy is linearly related to the external field strength. Further, strong fields effectively halt the cascade in the parallel direction and considerably inhibit the cascade in all other directions.

Finally, we have discovered that decaying EMHD turbulence yields a weak inverse cascade, at least partially transferring magnetic energy from intermediate to large length scales. The possibility of inverse cascades may have implications for the magnetic fields of neutron stars, where the proto-neutron star that emerges from a supernova explosion may well have a primarily small-scale, disordered field. A Hall-induced inverse cascade may then be a mechanism whereby it acquires a large-scale, ordered field. We note though that the electron number density n is strongly depth dependent in neutron stars, which turns out to interact with the Hall effect in a highly non-trivial way (Hollerbach and Rüdiger 2004; Vainshtein et al. 2000). It is likely therefore that both forward and inverse cascades will be rather different in real neutron stars than they are in isotropic, Cartesian box models such as here. Future work will consider EMHD in more realistic, stratified spherical-shell models.

References

Berger, M. A. 1997 *J. Geophys. Res.* **102**, 2637.

Biskamp, D., Schwarz, E. and Drake, J. F. 1996 *Phys. Rev. Lett.* **76**, 1264.

Biskamp, D., Schwarz, E., Zeiler, A., Celani, A. and Drake, J. 1999 *Phys. Plasmas* **6**, 751.

Biskamp, D. and Müller, W.-C. 1999 *Phys. Rev. Lett.* **83**, 2195–2198.

Cho, J. and Lazarian, A. 2004 *Astrophys. J.* **615**, L41.

Dastgeer, S., Das, A., Kaw, P. and Diamond, P. 2000 *Phys. Plasmas* **7**, 571.

Dastgeer, S. and Zank, G. P. 2003 *Astrophys. J.* **599**, 715.

Frigo, M. and Johnson, S. G. 2005 *Proc. IEEE* **93**, 216.

Galtier, S. 2006 *J. Plasma Phys.* **72**, 721.

Goldreich, P. and Reisenegger, A. 1992 *Astrophys. J.* **395**, 250–258.

Hollerbach, R. and Rüdiger, G. 2002 *Mon. Not. R. Astron. Soc.* **337**, 216.

Hollerbach, R. and Rüdiger, G. 2004 *Mon. Not. R. Astron. Soc.* **347**, 1237.

Iroshnikov, P. S. 1964 *Sov. Astron.* **7**, 566.

Kolmogorov, A. N. 1941 *Proc. USSR Acad. Sci.* **30**, 299 (in Russian); 1980 *Proc. R. Soc. A* **434**, 9 (in English).

Kraichnan, R. H. 1965 *Phys. Fluids* **8**, 1385

Kraichnan, R. H. 1967 *Phys. Fluids* **10**, 1417.

Oughton, S., Matthaeus, W. H. and Ghosh, S. 1998 *Phys. Plasmas* **5**, 4235.

Shaikh, D. and Zank, G. P. 2005 *Phys. Plasmas* **12**, 122310.

Shebalin, J. V., Matthaeus, W. H. and Montgomery, D. 1983 *J. Plasma Phys.* **29**, 525.

Vainshtein, S. I., Chitre, S. M. and Olinto, A. V. 2000 *Phys. Rev.* E **61**, 4422.

Wareing, C. J. and Hollerbach, R. 2009 *Phys. Plasmas* **16**, 042307 (RH09).